

## **Lin28 Regulates BMP4 and Functions with Oct4 to Affect Ovarian Tumor Microenvironment**

Wei Ma <sup>1,5\*</sup>, Jing Ma <sup>1,6\*</sup>, Jie Xu <sup>1</sup>, Chong Qiao <sup>1,7</sup>, Adam Branscum <sup>2</sup>, Andres Cardenas <sup>2</sup>, Andre T. Baron <sup>3,4</sup>, Peter Schwartz <sup>1</sup>, Nita J. Maihle <sup>1,8</sup>, and Yingqun Huang <sup>1</sup>

<sup>1</sup> Department of Obstetrics, Gynecology and Reproductive Sciences, Yale Stem Cell Center, Yale University School of Medicine, New Haven, Connecticut, USA

<sup>2</sup> Biostatistics Program, School of Biological and Population Health Sciences, Oregon State University, Corvallis, Oregon, USA

<sup>3</sup> Department of Epidemiology, University of Kentucky, Lexington, Kentucky, USA

<sup>4</sup> Department of Obstetrics and Gynecology, Division of Gynecologic Oncology, University of Kentucky, Lexington, Kentucky, USA

<sup>5</sup> Clinical Department, School of Medicine, Northwest University for Nationalities, Lanzhou, Gansu 730030, P. R. China

<sup>6</sup> Obstetrics and Gynecology Department, Third Xiangya Hospital of Central South University, Changsha, Hunan 410013, P. R. China

<sup>7</sup> Department of Obstetrics and Gynecology, Shengjing Hospital, China Medial University, Shengyang, Liaoning 110004, P. R. China

<sup>8</sup> Department of Pathology, Yale University School of Medicine, New Haven, Connecticut, USA.

\* These authors contributed equally to this work.

**Correspondence:** Yingqun Huang, M.D., Ph.D., Department of Obstetrics, Gynecology and Reproductive Sciences, Yale University School of Medicine, 310 Cedar Street, New Haven, CT 06510, USA; Email: [yingqun.huang@yale.edu](mailto:yingqun.huang@yale.edu)

**Running title:** Lin28/Oct4/BMP4 in ovarian cancer

## **Abstract**

Emerging evidence suggests that the tumor microenvironment plays a critical role in regulating cancer stem cells (CSCs) and tumor progression through both autocrine and paracrine signaling. Elevated production of bone morphogenetic proteins (BMPs) from human ovarian cancer cells and stroma has been shown to increase CSC proliferation and tumor growth. Here, we report that Lin28, a stem cell factor, binds to BMP4 mRNA in epithelial ovarian carcinoma cells thereby promoting BMP4 expression at the posttranscriptional level. As co-expression of Lin28 and Oct4 (another stem cell factor) has been implicated in ovarian cancer CSCs, we also determined that high levels of Lin28 are associated with an unfavorable prognosis when co-expressed with high levels of Oct4. Together, these findings uncover a new level of regulation of BMP4 expression, and imply a novel Lin28/Oct4/BMP4-mediated mechanism of regulating ovarian tumor cell growth, thus holding potential for the development of new strategies for the diagnosis and treatment of ovarian cancer.

## Introduction

Cancer stem cells (CSCs), by definition, have the ability to give rise to both more CSCs (by self-renewal) and daughter cells of other types (by differentiation); as a result these cells have the capacity to regenerate tumor cells. CSCs have been suggested to contribute to tumor recurrence, metastasis and the development of drug-resistance<sup>1-4</sup>. A recent series of paradigm-shifting studies suggests that cancer cells are highly plastic, and under certain conditions, can transition between cell types. For instance, differentiated non-CSCs can revert to CSCs, or vice versa – consistent with the view that the tumor microenvironment can reprogram any differentiated cell type into a CSC<sup>5-10</sup>. While such studies demonstrate the critical role of the tumor microenvironment in the development of the CSC phenotype, the factor(s) that give rise to this phenotype have not yet been identified.

The bone morphogenetic protein (BMP) family is under investigation as one potential family of growth factors controlling the growth of CSCs. BMPs belong to the transforming growth factor- $\beta$  (TGF- $\beta$ ) family of secretory peptides that regulate diverse cellular processes, including proliferation, differentiation, migration, adhesion and apoptosis (reviewed in<sup>11</sup>). BMP-mediated signal-transduction pathways play crucial roles in normal tissue development, maintaining tissue homeostasis, and tumorigenesis<sup>12</sup>. Approximately 20 BMP-related proteins have been identified; BMP2 and BMP4 are the best-studied members of this family. In particular, BMP2 and BMP4 are 91% identical at the protein level, bind to the same receptors, and likely function interchangeably (reviewed in<sup>12,13</sup>). Evidence that BMP2/4 plays critical roles in regulating ovarian CSCs comes from a recent study demonstrating that ovarian cancer-associated mesenchymal stem cells (CA-MSCs) exhibit elevated expression of both BMP2 and BMP4. Treatment of primary ovarian cancer cells or derived cell lines with exogenous BMP2 significantly stimulates proliferation of ovarian CSCs *in vitro* and tumor growth *in vivo*<sup>7</sup>. Further, inhibition of BMP2/4 by Noggin, an extracellular BMP inhibitor, results in partial abrogation of CA-MSC promoted tumor growth in mice<sup>7</sup>.

In addition to BMPs, specific stem cell factors such as Lin28 and Oct4 may contribute to

regulating ovarian CSCs and tumor progression<sup>14</sup>. Lin28 and Oct4 are co-expressed highly in undifferentiated human embryonic stem (ES) cells but not in most normal adult tissue cells, although aberrant activation of expression has been detected in diverse human malignancies (reviewed in<sup>15,16</sup>). Oct4 is a transcription factor that regulates expression of a network of genes essential for maintaining stem cell pluripotency<sup>17</sup>. Lin28 is an RNA-binding protein that functions to maintain stem cell viability and pluripotency through both blocking the biogenesis of let-7 family of miRNAs and promoting translation of mRNAs involved in cell growth and metabolism (reviewed in<sup>15,16</sup>). Further, Lin28 regulates Oct4 at the posttranscriptional level: in both human ES and EC (embryonic carcinoma) cells Lin28 specifically binds to Oct4 mRNA via recognition of a sequence element in the mRNA and stimulates its translation<sup>18</sup>. Intriguingly, co-expression of Lin28 and Oct4 also has been found in a sub-population of human epithelial ovarian carcinoma (EOC) cells and has been implicated in CSC function<sup>14</sup>. Importantly, reducing expression of both Lin28 and Oct4 simultaneously by siRNA-mediated gene silencing resulted in synergistic inhibition of cell growth and induction of apoptosis in EOC-derived cell lines<sup>14</sup>. However, the clinical impact of this co-expression is not known, despite the fact that this sub-population has been associated with high tumor grade in a 14-patient cohort<sup>14</sup>.

In this study, we identify BMP4 mRNA as a novel target of Lin28 regulation at the post-transcriptional level, revealing a new layer of complexity in regulation of BMP4 expression. We also demonstrate that co-expression of Lin28 and Oct4 negatively impacts patient survival. Together, these results imply Lin28-mediated BMP4 activation in the poor prognosis observed in a sub-population of ovarian cancer patients expressing high levels of both Lin28 and Oct4.

## **Results**

### **Lin28 associates with BMP4 mRNA in tumor cells**

Our recent studies on the expression of Lin28 and Oct4 in ovarian cancer suggested that these gene products might be involved in regulating factors that modulate the tumor microenvironment in epithelial

ovarian cancer (EOC). The identification of BMP2/4 as potent drivers of ovarian CSC growth and tumor progression<sup>7</sup> suggested to us that there might be a mechanistic link between Lin28 and BMP4.

As an RNA-binding protein, Lin28 is known to execute its function through binding to target RNAs in a form of ribonucleoprotein particles (RNPs) (reviewed in<sup>15</sup>). In previous studies we isolated Lin28-containing RNPs from human ES cells by immunoprecipitation (IP) using antibodies specific for Lin28, followed by identification of associated mRNAs using high throughput deep sequencing. We found approximately 5% of cellular mRNAs to be enriched greater than 2.5-fold (a threshold that defines a gene as a putative target of Lin28) in Lin28 IP versus control IP (preimmune serum)<sup>19</sup>. Importantly, a subset of mRNAs including those for HMGA1 and RPS13 (ribosomal protein S13) were subsequently validated to be Lin28 targets of regulation at the translational level<sup>19,20</sup>. Retrospective scrutiny of these genome-wide data suggested that BMP4 mRNA also was specifically enriched in the Lin28 IP fraction, and therefore warranted further investigation.

Figure 1A is a screenshot of normalized UCSF Genome Browser alignments of Lin28 IP and preimmune IP sequences, demonstrating a 3.9-fold enrichment of BMP4 mRNA in Lin28-containing RNPs in human ES cells<sup>19</sup>. To determine whether BMP4 mRNA also is bound by Lin28 in tumor cells, IP experiments were carried out using human ovarian teratocarcinoma-derived PA-1 cells, which endogenously express high levels of Lin28<sup>14,18,19</sup>, followed by RNA extraction and reverse transcription and quantitative real-time PCR (RT-qPCR). Figure 1B illustrates the mRNA levels present in Lin28-containing RNPs (red bars) compared to those identified using a rabbit pre-immune serum (blue bars; arbitrarily set as 1). While the known Lin28 targets Hmga1 and Rps13 were enriched by ~5- and 30-fold, respectively, in Lin28 IP vs. preimmune IP (2<sup>nd</sup> and 3<sup>rd</sup> columns from left, compare red bar with blue bar), the non-target beta-actin mRNA was not (1<sup>st</sup> column from right). Importantly, under the same conditions Bmp4 was also enriched, by nearly 7-fold (1<sup>st</sup> column from left). Significant enrichment of Bmp4, Hmga1, and Rps13 in Lin28 RNPs also was observed in the human EOC-derived line IGROV1 (Fig. 1C, 1<sup>st</sup> through 3<sup>rd</sup> columns from left); this cell line previously has been shown to express

endogenous Lin28, albeit at much lower levels when compared to PA-1<sup>14</sup>. Together these observations support the hypothesis that BMP4 mRNA is physically associated with Lin28 in EOC-derived lines.

### **Lin28 stimulates BMP4 expression at the posttranscriptional level**

Based on our previous studies showing that Lin28 enhances the translation of a number of its target mRNAs<sup>18-21</sup> we proposed that Lin28 might also influence BMP4 expression in a similar fashion. To test this hypothesis we first asked whether increasing Lin28 levels in EOC-derived cell lines that express low levels of endogenous Lin28 would lead to elevated BMP4 expression. We transfected an epitope-tagged Lin28 expression vector (FL-Lin28)<sup>19</sup> into IGROV1 cells, followed by analysis of BMP4 expression. To facilitate measurement of BMP4 protein levels, we treated cells with the protein transport inhibitor GolgiPlug<sup>7</sup> to block BMP4 secretion prior to total cellular protein extraction and immunoblotting analysis. Under these conditions we observed an approximately 3-fold increase in BMP4 protein expression in cells transfected with FL-Lin28 compared to empty vector (Fig. 2A, top panel, top blot, compare lane 2 to lane 1). The level of FL-Lin28 expression was ~15-fold higher than that of endogenous Lin28 (Fig. 2A, top panel, 2<sup>nd</sup> blot from the top, compare the top to the bottom band in lane 2). However, no change in BMP4 mRNA expression was observed in response to FL-Lin28 expression (Fig. 2A, bottom panel, compare red bar with blue bar in the 1<sup>st</sup> column from left). Similar results were obtained when a second EOC-derived cell line, A2780, was tested. A2780 cells express negligible levels of endogenous BMP4 and Lin28 (Fig. 2B, top panel, the 1<sup>st</sup> and 2<sup>nd</sup> blots from top in lane 1). When FL-Lin28 was expressed exogenously (Fig. 2B, top panel, 2<sup>nd</sup> blot from the top, lane 2), the level of BMP4 protein expression becomes readily detectable (Fig. 2B, top panel, top blot, lane 2), even though BMP4 mRNA levels are not significantly affected (Fig. 2B, bottom panel). Next, we asked whether decreasing Lin28 expression in PA-1 cells that express robust levels of endogenous Lin28 would result in reduced BMP4 production. Thus, PA-1 cells were transfected with a control siRNA (siCon) or Lin28-specific siRNA (siLin28)<sup>18,19,21</sup> and the effect on BMP4 expression was analyzed. The

level of Lin28 mRNA in siLin28-transfected cells was reduced by 98% compared to siCon-transfected cells (Fig. 2C, bottom panel, 1<sup>st</sup> column from left, compare red bar with purple bar), with a concomitant ~4-fold decrease in the Lin28 protein level (top panel, 2<sup>nd</sup> blot from top, compare lane 2 to lane 1). Concomitant with this down-regulation of Lin28, the level of BMP4 protein expression was decreased by half (Fig. 2C, top panel, top blot, compare lane 2 to lane 1), again without a significant change in BMP4 mRNA levels (bottom panel, middle column, compare red bar with purple bar). Together, Lin28 expression positively influences BMP4 at the protein level without affecting its mRNA, suggesting that BMP4 is likely regulated by Lin28 at the translational level.

To further investigate whether Lin28 might regulate BMP4 mRNA translation, we asked whether BMP4 mRNA contains the sequence element recognized by Lin28, thus enabling Lin28-dependent translational regulation. We previously have reported that multiple Lin28 mRNA targets share a unique sequence and structural motif that is recognized by Lin28 and that enables Lin28-dependent stimulation of translation<sup>20</sup>. This motif is characterized by a small “A” bulge flanked by two G:C base-pairs embedded in a complex secondary structure<sup>20</sup>. Using the same bioinformatics approach combined with a heterologous reporter system we identified a 411-nt long Lin28-responsive element (LRE) in the coding region of BMP4 that possesses such properties (Fig. 2D, top panel, blue rectangle, and Supplementary Fig. S1). When this LRE was inserted at the 3'-UTR of a well-characterized firefly luciferase (FFL) reporter gene<sup>18-21</sup>, it conveyed dose-dependent stimulation of translation by Lin28. We used as a positive control a 129-nt LRE from Hmga1<sup>20</sup> (Fig. 2D, bottom panel, yellow line), and found stimulatory effects similar to those observed using the 411-nt LRE region of Bmp4 (blue line); in comparison, neither the mutant Hmga1 element (Hmga1-53T, which contains an “A” to “T” single point mutation<sup>20</sup>, purple line) nor the parental FFL (red line) showed such a stimulatory effect. Together, these results strongly suggest that BMP4 is regulated by Lin28 at the translational level via binding to a discrete LRE. More detailed analyses will be needed to confirm this interpretation of these results.

## **Co-expression of Lin28 and Oct4 is associated with unfavorable prognosis**

In light of the observation that Lin28 can promote BMP4 production via a canonical post-transcriptional regulatory mechanism, and also because BMP4 has been implicated in playing a critical role in ovarian CSC control as well as the pathogenesis of ovarian cancer<sup>7,22-26</sup>, we were motivated to determine, using immunohistochemical methods, whether expression of Lin28, together with Oct4, might be correlated with clinical outcome in EOC patients. The rationale for including Oct4 was based on two previous observations. First, co-expression of Lin28 and Oct4 in ovarian cancer cells is associated with increased tumor grade, and second, silencing the expression of both Lin28 and Oct4 results in synergistic inhibition of ovarian cancer cell growth and induction of apoptosis<sup>14</sup>. Because BMP4 is a secreted protein, it is not possible to determine the precise compartment(s) (i.e., tumor cells, stroma, or both) from which this protein arises in ovarian tumor tissue samples using immunohistochemistry. In contrast, Lin28 is a cytoplasmic protein that is expressed exclusively in the ovarian tumor cell compartment (see below). The fact that BMP4 can be expressed from either compartment but Lin28 is only in tumor cells thus creates limitations that precluded us from performing co-localization studies with BMP4 without confounding interpretations. Since expression of BMP2 (which binds to the same receptors of BMP4) has already been shown to be a prognostic factor in epithelial ovarian cancer<sup>25</sup>, and since BMP2 and BMP4 are likely functionally interchangeable<sup>7,13</sup>, we set out to study the potential relationship between Lin28/Oct4 expression and outcome in ovarian cancer. Expression of Lin28 and Oct4 was examined using immunofluorescence microscopy using paraffin-embedded tumor (primary) samples from 343 patients in the Yale Ovarian Cancer Cohort (Supplementary Table S1). The Lin28 and Oct4 antibodies used in these studies have been well documented previously for specificity in detecting their respective antigens by immunoblot analysis<sup>14,18,19</sup>. Lin28 and Oct4 protein levels were determined using the Automated Quantitative Analysis (AQUA) method<sup>27,28</sup>. The distribution of both Lin28 and Oct4 scores is summarized in Figure 3A. A heterogeneous pattern of expression across tumor samples was observed for both Lin28 and Oct4. The AQUA scores of Lin28 ranged from 0 (undetectable values) to 4889.49,

with mean and median values of 668.16 and 504.98, respectively. In the case of Oct4, the AQUA scores ranged from 0 to 1063.58, with mean and median values of 110.22 and 87.88, respectively. For both Lin28 and Oct4, most expression was detected in co-localization with cells expressing cytokeratin, which defines epithelially-derived tumor cells; staining was not detected in nearby stromal cells. All Lin28/Oct4-positive histospots expressed Lin28/Oct4 homogeneously within the cytokeratin-staining compartment. Figure 3B shows representative images of histospots expressing high levels of both Lin28 and Oct4. Consistent with the previously described localization of these two proteins in human ES and EC cells <sup>14,18</sup>, the expression patterns of Lin28 (panels I-IV) and Oct4 (Panels V-VIII) are predominantly cytoplasmic and nuclear, respectively.

Among the various clinico-/pathologic factors analyzed in the Yale Ovarian Cancer Cohort, age and stage were both predictably found to be independent risk factors for predicting progression free survival (PFS) and overall survival (OS) (Supplementary Table S2, Multivariate Model,  $p < 0.001$  for both PFS and OS by age, and  $p < 0.001$  for PFS by stage). While neither Lin28 nor Oct4 expression alone showed significant association with survival, there was evidence of an interaction between Lin28 and Oct4 that is significant in predicting both PFS and OS (Supplementary Table S2,  $p = 0.038$  for PFS, and  $0.036$  for OS). To determine the nature of this interaction, multivariate analyses for PFS and OS were compared among patients with no, medium, or high Lin28 expression levels, and no, medium or high Oct4 expression levels. As shown in Supplementary Table S3, odds ratios and hazard ratios suggested that patients with high levels of Lin28 and Oct4 co-expressed in their tumors (double high) had the least favorable PFS and OS, in comparison to other 8 groups (i.e., High Lin28/No Oct4, No Lin28/High Oct4, High Lin28/Medium Oct4, Medium Lin28/High Oct4, Medium Lin28/Medium Oct4, Medium Lin28/No Oct4, No Lin28/Medium Oct4, and No Lin28/No Oct4). The survival curves illustrate that in the group of patients with high Lin28 expression, those with high Oct4 had worse survival than those with only high Lin28 ( $p = 0.014$ ) or high Oct4 ( $p = 0.003$ ) (Fig. 3C, left panel). Intriguingly, patients with no Lin28 and no Oct4 expression (double negative) also had worse survival

than those with only high Lin28 ( $p=0.039$ ) or high Oct4 ( $p=0.009$ ), while no significant difference between the double negative and double high groups was found ( $p=0.075$ ) (Fig. 3C, right panel). Importantly, these relationships remain significant after adjustment for other risk factors, including age, stage, grade, histology, bilateral involvement (BOI) and category. Together, these results suggest that Lin28, in combination with Oct4, may represent a new and independent prognostic marker for ovarian cancer.

## **Discussion**

In this report, we demonstrate that the stem cell factor Lin28 not only physically interacts with BMP4 mRNA (Fig. 1) but also stimulates BMP4 expression, we hypothesize, at the translational level (Fig. 2), in human EOC-derived cell lines. We also have mapped a Lin28-responsive element (LRE) within the coding region of BMP4 mRNA that confers Lin28-dependent stimulation of translation using a heterologous reporter system (Fig. 2D). Like other BMP family members, the activity of BMP4 as a secreted growth factor can be regulated at multiple levels including through the binding of soluble extracellular inhibitors, receptor oligomerization, endocytosis, and co-receptor association (reviewed in <sup>11</sup>). In addition, epigenetic methylation of the promoter has been reported to affect BMP4 expression at the transcriptional level <sup>29</sup>. Here we propose that Lin28 regulates BMP4 expression at the translational level, adding another layer of complexity to the regulation of BMP4 expression.

Both BMP4 and BMP2 have been shown to be critical in regulating the ovarian tumor microenvironment, and in so doing, tumor progression. Shepherd et al <sup>22</sup> reported that BMP4 secreted from ovarian cancer cells up-regulates the expression of the proto-oncogene inhibitor of differentiation 3 (ID3) in an autocrine fashion, thereby driving tumorigenesis. Autocrine BMP4 signaling also has been shown to induce epithelial-mesenchymal transition (EMT), and to increase adhesion, motility, and invasion of ovarian cancer cells <sup>23</sup>. Similarly, up-regulation of BMP2 has been observed in ovarian cancer cells compared to normal ovarian surface epithelial cells, which are considered one potential

progenitor cell type of epithelial ovarian cancer (EOC)<sup>24</sup>. In addition, elevated expression of BMP2 in ovarian tumors has been associated with poor prognosis<sup>25</sup>. The important role of BMPs in ovarian tumorigenesis is further supported by the observation that chordin, an extracellular BMP inhibitor, is downregulated in ovarian cancer cells compared to ovarian surface epithelial cells<sup>26</sup>. Finally, a recent study has elegantly demonstrated that 1) ovarian carcinoma-associated mesenchymal stem cells (CA-MSCs) are able to promote tumor growth more effectively than MSCs from healthy individuals in co-culture experiments both *in vitro* and in a mouse model; and that 2) CA-MSCs secrete significantly higher levels of BMP2 and BMP4, compared to control MSCs; 3) treatment of primary ovarian cancer cells or ovarian cancer-derived cell lines with BMP2 significantly increases the number of CSCs; and 4) *in vitro* and *in vivo* inhibition of BMP2/4 by Noggin (an extracellular BMP inhibitor) results in partial abrogation of CA-MSC promoted tumor growth<sup>7</sup>. Collectively, these studies highlight the role of BMP2/4-mediated autocrine and paracrine signaling pathways in regulating the growth of human ovarian cancer cells. It is noteworthy that BMP4 also has been reported to induce differentiation and apoptosis of CSCs from glioma and colorectal cancer<sup>30,31</sup>, in contrast to the situation where CA-MSC-derived BMP2/4 promotes proliferation of CSCs in ovarian cancer<sup>7</sup>. This discrepancy provides further support for the notion that the physiological endpoints of BMP-mediated regulation are highly context-dependent<sup>11,12</sup>. Indeed, distinct and cell-type-specific effects of BMP4 have been reported<sup>32</sup>. In this regard, high levels of Lin28 expression have been observed in extraembryonic endoderm, in addition to undifferentiated ES cells, suggesting a role for Lin28 in extraembryonic endoderm differentiation<sup>33</sup>. Importantly, BMP4 signaling is known to support differentiation of ES cells into both embryonic and extraembryonic lineages<sup>34,35</sup>. We suspect that the interaction between Lin28 and BMP4 mRNA detected in extracts prepared from human ES cells (Fig. 1A and<sup>19</sup>) reflects the presence of a subpopulation of differentiating cells, rather than being a function of undifferentiated ES cells.

The regulation of BMP4 expression by Lin28, as well as our previous studies linking Lin28 and Oct4 to ovarian cancer cell growth stimulated us to examine potential clinical correlates of these

observations. In these studies we found no correlation between Lin28 or Oct4 expression alone and patient survival, consistent with one previous report demonstrating that high Lin28B, but not Lin28, is correlated with shorter PFS and OS in ovarian cancer patients<sup>36</sup>. We also observed a statistically significant relationship between high Lin28 expression and high Oct4 expression (double high), and the risk of disease progression and death. Specifically, patients in the double high cohort showed decreased PFS and OS in comparison to patients with other combinations of Lin28/Oct4 expression (Supplementary Table S3, and Fig. 3C, left panel). This observation is consonant with our previous observation demonstrating that Lin28 and Oct4 are co-expressed in a sub-population of EOC cells in ovarian cancer-derived cell lines (as well as in a small cohort of tumor samples), and that simultaneous silencing of the expression of both these proteins synergistically inhibits ovarian cancer cell growth and survival<sup>14</sup>. It is intriguing that patients in the double negative cohort also showed significantly poor prognosis (Fig. 3C, right panel), reminiscent of patients with ER/PR/HER2-triple negative breast cancer. It is likely that the double high and the double negative groups represent distinct underlying mechanisms. Indeed, it has been reported that Lin28, and its paralog Lin28B, are mutually exclusively expressed in HER2-overexpressing and triple-negative breast cancer, respectively, and that the NF- $\kappa$ B transcription factor regulates Lin28B (but not Lin28)-mediated inflammatory circuit in the triple negative breast cancer<sup>37</sup>. Future investigations will illuminate distinct mechanisms underlying the double high and the double negative ovarian tumors, which will be useful in customizing treatment for ovarian cancer patients.

We elected not to perform co-staining with BMP4 on ovarian tumor samples due to the challenges associated with data interpretation for this secreted protein. However, its close relative BMP2, which acts via the same receptors as BMP4, and which often functions in parallel or perhaps even interchangeably with BMP4<sup>7,13</sup>, previously has been shown to independently be correlated with survival in ovarian cancer, despite the observation that the precise compartment(s) from which BMP2 is expressed in ovarian tumor samples cannot be determined using immunohistochemistry<sup>25</sup>. Despite

these limitations, we propose here that the results from our *in vivo* Lin28 and Oct4 tumor expression studies, combined with our *in vitro* results, provide potential new links revealing functional interactions among Lin28, Oct4, and BMP4 - links which may be relevant to ovarian cancer pathogenesis.

Specifically, we hypothesize that the Lin28/Oct4-double high EOC cells may represent a sub-population of tumor cells that contributes critically to disease progression (Fig. 4). These cells are capable of producing high levels of BMP4 partly under the influence of Lin28; this growth factor, in turn, stimulates CSC proliferation in a paracrine fashion. In addition, BMPs derived from ovarian carcinoma-associated mesenchymal stem cells (CA-MSCs) also may stimulate CSC proliferation<sup>7</sup>. One important question that remains is whether CSCs promote their own growth through autocrine signaling mechanisms, and if so, which growth factors are involved. In this context, the possibility that BMP4 may also regulate Lin 28 expression is an intriguing possibility that warrants further study.

## **Materials and Methods**

### **Antibodies and DNA plasmids**

The antibodies specific for Lin28 (Abcam, ab46020), Oct4 (Santa Cruz, sc-5279), cytokeratin (DAKO, M351501-2), BMP4 (Abcam, ab39973), beta-tubulin (Abcam, ab6046), rabbit pre-immune serum (SouthernBiotech, 0040-01) and mouse pre-immune IgG (Chemicon PP54) were purchased. The plasmids FL-Lin28, FFL, Hmga1-129, and Hmga1-53T were previously described<sup>18-21</sup>. The Bmp4-411 plasmid was made by cloning a PCR fragment containing the 411-nt BMP4 sequence (nt 845 to nt 1255 relative to the transcriptional start site of human BMP4, NM\_001202) at the NotI and XhoI sites of the parental FFL reporter gene. A cDNA from PA-1 cells (as a template for the BMP4 gene) and a pair of forward (5'-AAGGAAAAAAGCGGCCGCTaacctcagcagcatccctga) and reverse (5'-CCGCTCGAGccatcatggccaaaggtgacca) primers were used in the PCR reactions.

### **Cell culture and transfection**

The culture and transfection of the human ovarian cancer-derived cell lines IGROV1 and A2870 and the human EC-derived PA-1 were carried out as previously described<sup>14,19</sup>.

### **Immunoprecipitation, deep sequencing, and RT-qPCR**

These were carried out essentially as previously described<sup>18,19</sup>. The PCR primers are listed below.

Beta-actin forward: 5'-ATCAAGATCATTGCTCCTCCTGAG; beta-actin reverse: 5'-

CTGCTTGCTGATCCACATCTG; beta-tubulin forward: 5'-CGTGTTTCGGCCAGAGTGGTGC; beta-

tubulin reverse: 5'-GGGTGAGGGCATGACGCTGAA; Bmp4 forward: 5'-

GTGGAGGAAGCTGACAACAA; Bmp4 reverse: 5'-GCCGGTTACAGAACCACACT; Lin28

forward: 5'-CGGGCATCTGTAAGTGGTTC; Lin28 reverse: 5'-CAGACCCTTGGCTGACTTCT;

Rps13 forward: 5'-CTCTCCTTTCGTTGCCTGAT; Rps13 reverse: 5'-

CCCTTCTTGGCCAGTTTGTA; Hmga1 forward: 5'-CAGCGAAGTGCCAACACCTAAG; Hmga1

reverse: 5'-CCTTGGTTTCCTTCCTGGAGTT; FFL forward: 5'-GCTGGGCGTTAATCAGAGAG;

FFL reverse: 5'-GTGTTCGTCTTCGTCCCAGT.

### **Luciferase assays**

These were carried out as previously described<sup>18-20</sup>.

### **Case selection and tissue annotation**

Three hundred and forty-three cases with ovarian pathology were identified from the Yale Pathology Archives to create a tissue microarray (TMA) in accordance with an Internal Review Board approved protocol. All patients had received primary surgery for an adnexal tumor at the Yale University School of Medicine between 1980 and 2001. Demographical, anthropomorphical, and clinicopathological parameters were collected from tumor registry data and through a detailed chart review of each case represented on the TMA. Demographical and anthropomorphical parameters included: date of birth,

race, gravidity, parity, hormone replacement therapy, body surface area in square meters, and smoking history. Clinicopathological parameters included: date of diagnosis, clinical diagnosis (e.g., epithelial ovarian cancer [EOC], non-epithelial ovarian cancer, low malignant potential ovarian tumor [LMP], benign ovarian tumor, fallopian tube cancer, and other gynecological cancer or non-gynecological cancer with metastasis to the ovary), other cancer (i.e., synchronous or metachronous secondary cancers), serum CA125 value (Units/ml) at the time of diagnosis, International Federation of Gynecology and Obstetrics (FIGO) disease stage, tumor grade and histological subtype (i.e., serous, mucinous, endometrioid, clear cell, transitional, mixed, other), presence of ascites, number of lymph nodes positive for cancer, number of lymph nodes removed at surgery, maximum non-omental tumor size, residual tumor following surgery, bilateral ovarian involvement (BOI), date of surgery, date of first chemotherapy or radiation therapy, neoadjuvant therapy, type of adjuvant chemotherapy (e.g., doxorubicin with platinum, paclitaxel with platinum, and cyclophosphamide with platinum), date of recurrence, date last seen, and vital status.

### **Tissue microarrays**

TMA construction was performed by the Yale University, Tissue Microarray Facility using paraffin-embedded tissue blocks as previously described<sup>38</sup>. Briefly, 0.6 mm diameter tissue cores of ovarian tumor tissue were spaced 0.8 mm apart on a recipient block using a precision instrument (Beecher, Silver Spring, MD), re-embedded in paraffin, and stored in a nitrogen chamber at room temperature. Duplicate cores of 17 ovarian tumors were included on the TMA as internal controls.

### **Immunohistochemistry (IHC)**

Immunohistochemical staining of TMA slides was carried out essentially as previously described<sup>38</sup>. The anti-Lin28 (protein A sepharose affinity purified), anti-Oct4, and anti-cytokeratin antibodies were used at dilutions of 1:600, 1:200, and 1:100, respectively. Protein A sepharose affinity purified rabbit

and mouse pre-immune IgGs at the same IgG concentrations were used as negative controls for these antibodies, respectively.

### **Automated quantitative analysis (AQUA)**

Automated quantitative analysis (AQUA) is a method that enables objective measurement of exact protein concentration within a defined tumor area or subcellular compartment<sup>28</sup>. Using an Olympus AX-51 epifluorescent microscope and an algorithm for image collection<sup>27</sup>, a series of monochromatic high-resolution images were captured. For each histospot an in- and out-of-focus image were acquired using the signals from the Lin28 (or Oct4)-Cy5 and cytokeratin-Alexa 488 channel, respectively. Based on the cytokeratin signal a tumor mask representing epithelial tumor compartment and excluding stromal, lymphocytic and histocytic areas was created. Only signal within the tumor mask was accounted for a positive score. AQUA scores of each histospot were generated by dividing the signal intensity by the area of the tumor mask.

### **Statistical analysis**

Exploratory data analysis: Statistical analyses were performed using Stata version 12 (Stata Corp, College Station, Texas) or SAS version 9.3 (Statistical Analysis Software Institute, Cary, NC). To define a cohort amenable to progression-free survival (PFS) and overall survival (OS) analysis, the descriptive statistics of all demographical, anthropomorphical, clinicopathological, and IHC parameters for all 404 cases represented in the TMA were first examined. Parameters with a high percentage of missing data values and subgroups with a small numbers of cases were eliminated for further study as potential prognostic factors. For example, race was eliminated as a potential prognosticator, because there were only 7 African American and 16 other, non-Caucasian patients among the cases. In addition, EOC patients who had received neo-adjuvant therapy (n=14) were eliminated from analysis of PFS and OS, because of potential treatment effects on Lin28 and Oct4 tissue expression. The assessment of

potential prognostic factors, therefore, was reduced to a cohort of 343 patients with primary EOC (n=285), fallopian tube cancer (n=16), low malignant potential (LMP) ovarian tumors (n=5), non-gynecologic (n=15) and other gynecologic (n=22) malignancies that had metastasized to the ovary. To accommodate valid comparisons of univariate and multivariate regression models, this cohort was annotated with a final list of covariates that included: category of specimen (see Table S1), age at diagnosis, disease stage, tumor grade, tumor histology, Bilateral Involvement (BOI), and IHC labeling of Lin28 and Oct4.

Spearman's rank correlation analysis was used to test for relationships between continuous covariates, and hence to reveal any potential confounders of a prognostic relationship. In addition, mean IHC labeling of Lin28 and Oct4 was compared across categories of disease stage, tumor grade, tumor histology, BOI, and category of specimen to identify significant associations between these covariates by Wilcoxon rank-sum or Kruskal-Wallis tests.

Survival analysis: Progression-free survival was defined as the date of surgery until the date of first clinically recognizable evidence of local or distant recurrence. Both left (n=70) and right (n=108) censoring was observed for PFS. Patients were left censored if they died of EOC, but the date of disease recurrence was unknown. Patients were right censored if they had no evidence of cancer recurrence at the last date seen alive. To accommodate left censoring, a parametric accelerated failure time (AFT) regression model with a log-logistic distribution function was used to fit covariates for PFS<sup>39</sup>. The log-logistic distribution was chosen because it may be characterized by an exponentially decreasing survival probability function, which is conceptually plausible as recurrence of disease is most likely to occur soon after surgery among patients with more advanced stage disease and/or aggressive tumors. In addition, the log-logistic AFT model facilitates the interpretation of transformed regression coefficients as odds ratios. Both univariate and multivariate AFT models of PFS were developed with the following covariates: patient age as a continuous variable, disease stage, tumor grade, tumor histology (serous vs.

all other subtypes), BOI, and IHC labeling of Lin28 and Oct4.

Overall survival is defined as the date of surgery until the date of death or loss to follow-up. Since only right censoring was observed for OS (n=201), multivariate Cox proportional hazard regression analysis<sup>40</sup> was used to fit patient age as a continuous variable, disease stage, tumor grade, tumor histology (serous vs. all other subtypes), BOI, and IHC labeling of Lin28 and Oct4 to OS. Analysis of Schoenfeld residuals along with univariate and global tests of the proportional hazards assumption using time-dependent covariates demonstrated that the hazard of dying is not proportional across stage I, II, III, and IV (data not shown). Therefore, data were stratified by disease stage in multivariate Cox regression models for overall survival.

Exploratory multivariate AFT and stratified Cox regression modeling demonstrated the existence of a significant interaction between Lin28 and Oct4. A backward stepwise elimination procedure was used to develop final multivariate AFT and Cox regression models for PFS and OS, respectively. All statistical tests were two-sided and considered significant with a p-value  $\leq 0.05$ .

### **Acknowledgements**

We would like to thank David Rimm for sharing expertise, reagents, and analytic tools related to AQUA, Setsuko Chambers and Wenxin Zheng for their development of the TMA used in these studies, and Richard Hochberg and Lingeng Lu for critical reading of the manuscript. This work was supported by a 09SCAYALE14 Connecticut Stem Cell Grant and a 1063338 Albert McKern Scholar Award to Y.H., and a Yale School of Medicine ‘Senior Women in Medicine’ Professorship to N.J.M.

All authors declare no conflicts of interest associated with this work.

## References

1. Nguyen LV, Vanner R, Dirks P, Eaves CJ. Cancer stem cells: an evolving concept. *Nat Rev Cancer* 2012; 12:133-43.
2. Chen J, Li Y, Yu TS, McKay RM, Burns DK, Kernie SG, et al. A restricted cell population propagates glioblastoma growth after chemotherapy. *Nature* 2012; 488:522-6.
3. Driessens G, Beck B, Caauwe A, Simons BD, Blanpain C. Defining the mode of tumour growth by clonal analysis. *Nature* 2012; 488:527-30.
4. Schepers AG, Snippert HJ, Stange DE, van den Born M, van Es JH, van de Wetering M, et al. Lineage tracing reveals Lgr5+ stem cell activity in mouse intestinal adenomas. *Science* 2012; 337:730-5.
5. Chaffer CL, Brueckmann I, Scheel C, Kaestli AJ, Wiggins PA, Rodrigues LO, et al. Normal and neoplastic nonstem cells can spontaneously convert to a stem-like state. *Proc Natl Acad Sci U S A* 2011; 108:7950-5.
6. Gupta PB, Fillmore CM, Jiang G, Shapira SD, Tao K, Kuperwasser C, et al. Stochastic state transitions give rise to phenotypic equilibrium in populations of cancer cells. *Cell* 2011; 146:633-44.
7. McLean K, Gong Y, Choi Y, Deng N, Yang K, Bai S, et al. Human ovarian carcinoma-associated mesenchymal stem cells regulate cancer stem cells and tumorigenesis via altered BMP production. *J Clin Invest* 2011; 121:3206-19.
8. Booth BW, Mack DL, Androutsellis-Theotokis A, McKay RD, Boulanger CA, Smith GH. The mammary microenvironment alters the differentiation repertoire of neural stem cells. *Proc Natl Acad Sci U S A* 2008; 105:14891-6.
9. Scheel C, Eaton EN, Li SH, Chaffer CL, Reinhardt F, Kah KJ, et al. Paracrine and autocrine signals induce and maintain mesenchymal and stem cell states in the breast. *Cell* 2011; 145:926-40.
10. Meyer MJ, Fleming JM, Ali MA, Pesesky MW, Ginsburg E, Vonderhaar BK. Dynamic regulation of CD24 and the invasive, CD44posCD24neg phenotype in breast cancer cell lines. *Breast Cancer Res* 2009; 11:R82.

11. Ehrlich M, Horbelt D, Marom B, Knaus P, Henis YI. Homomeric and heteromeric complexes among TGF-beta and BMP receptors and their roles in signaling. *Cell Signal* 2011; 23:1424-32.
12. Miyazono K, Kamiya Y, Morikawa M. Bone morphogenetic protein receptors and signal transduction. *J Biochem* 2010; 147:35-51.
13. Kawabata M, Imamura T, Miyazono K. Signal transduction by bone morphogenetic proteins. *Cytokine Growth Factor Rev* 1998; 9:49-61.
14. Peng S, Maihle NJ, Huang Y. Pluripotency factors Lin28 and Oct4 identify a sub-population of stem cell-like cells in ovarian cancer. *Oncogene* 2010; 29:2153-9.
15. Huang Y. A mirror of two faces: Lin28 as a master regulator of both miRNA and mRNA. *Wiley Interdiscip Rev RNA* 2012.
16. Thornton JE, Gregory RI. How does Lin28 let-7 control development and disease? *Trends Cell Biol* 2012.
17. Pei D. Regulation of pluripotency and reprogramming by transcription factors. *J Biol Chem* 2009; 284:3365-9.
18. Qiu C, Ma Y, Wang J, Peng S, Huang Y. Lin28-mediated post-transcriptional regulation of Oct4 expression in human embryonic stem cells. *Nucleic Acids Res* 2010; 38:1240-8.
19. Peng S, Chen LL, Lei XX, Yang L, Lin H, Carmichael GG, et al. Genome-wide Studies Reveal that Lin28 Enhances the Translation of Genes Important for Growth and Survival of Human Embryonic Stem Cells. *Stem Cells* 2011; 29:496-504.
20. Lei XX, Xu J, Ma W, Qiao C, Newman MA, Hammond SM, et al. Determinants of mRNA recognition and translation regulation by Lin28. *Nucleic Acids Res* 2011.
21. Jin J, Jing W, Lei XX, Feng C, Peng S, Boris-Lawrie K, et al. Evidence that Lin28 stimulates translation by recruiting RNA helicase A to polysomes. *Nucleic Acids Res* 2011.
22. Shepherd TG, Theriault BL, Nachtigal MW. Autocrine BMP4 signalling regulates ID3 proto-oncogene expression in human ovarian cancer cells. *Gene* 2008; 414:95-105.

23. Theriault BL, Shepherd TG, Mujoomdar ML, Nachtigal MW. BMP4 induces EMT and Rho GTPase activation in human ovarian cancer cells. *Carcinogenesis* 2007; 28:1153-62.
24. Theriault BL, Shepherd TG. On the path to translation: Highlights from the 2010 Canadian Conference on Ovarian Cancer Research. *J Ovarian Res* 2011; 4:10.
25. Le Page C, Puiffe ML, Meunier L, Zietarska M, de Ladurantaye M, Tonin PN, et al. BMP-2 signaling in ovarian cancer and its association with poor prognosis. *J Ovarian Res* 2009; 2:4.
26. Moll F, Millet C, Noel D, Orsetti B, Bardin A, Katsaros D, et al. Chordin is underexpressed in ovarian tumors and reduces tumor cell motility. *FASEB J* 2006; 20:240-50.
27. Camp RL, Chung GG, Rimm DL. Automated subcellular localization and quantification of protein expression in tissue microarrays. *Nat Med* 2002; 8:1323-7.
28. Moeder CB, Giltnane JM, Moulis SP, Rimm DL. Quantitative, fluorescence-based in-situ assessment of protein expression. *Methods Mol Biol* 2009; 520:163-75.
29. Lucio-Eterovic AK, Singh MM, Gardner JE, Veerappan CS, Rice JC, Carpenter PB. Role for the nuclear receptor-binding SET domain protein 1 (NSD1) methyltransferase in coordinating lysine 36 methylation at histone 3 with RNA polymerase II function. *Proc Natl Acad Sci U S A* 2010; 107:16952-7.
30. Zhou Z, Sun L, Wang Y, Wu Z, Geng J, Miu W, et al. Bone morphogenetic protein 4 inhibits cell proliferation and induces apoptosis in glioma stem cells. *Cancer Biother Radiopharm* 2011; 26:77-83.
31. Lombardo Y, Scopelliti A, Cammareri P, Todaro M, Iovino F, Ricci-Vitiani L, et al. Bone morphogenetic protein 4 induces differentiation of colorectal cancer stem cells and increases their response to chemotherapy in mice. *Gastroenterology* 2011; 140:297-309.
32. Fessing MY, Atoyan R, Shander B, Mardaryev AN, Botchkarev VV, Jr., Poterlowicz K, et al. BMP signaling induces cell-type-specific changes in gene expression programs of human keratinocytes and fibroblasts. *J Invest Dermatol* 2010; 130:398-404.
33. Darr H & Benvenisty N. Genetic analysis of the role of the reprogramming gene LIN-28 in human

embryonic stem cells. *Stem Cells* 2009; 27:352-362.

34. Xu RH, Chen X, Li DS, Li R, Addicks GC, Glennon C, et al. BMP4 initiates human embryonic stem cell differentiation to trophoblast. *Nat Biotechnol* 2002; 20:1261-1264.

35. Zhang P, Ku J, Tan Z, Wang C, Liu T, Chen L, et al. Short-term BMP-4 treatment initiates mesoderm induction in human embryonic stem cells. *Blood* 2008;111:1933-1941.

36. Lu L, Katsaros D, Shaverdashvili K, Qian B, Wu Y, de la Longrais IA, et al. Pluripotent factor lin-28 and its homologue lin-28b in epithelial ovarian cancer and their associations with disease outcomes and expression of let-7a and IGF-II. *Eur J Cancer* 2009; 45:2212-8.

37. Piskounova E, Polytarchou C, Thornton JE, LaPierre RJ, Pothoulakis C, Hagan JP, et al. Lin28A and Lin28B inhibit let-7 microRNA biogenesis by distinct mechanisms. *Cell* 2011; 147:1066-79.

38. Camp RL, Dolled-Filhart M, King BL, Rimm DL. Quantitative analysis of breast cancer tissue microarrays shows that both high and normal levels of HER2 expression are associated with poor outcome. *Cancer Res* 2003; 63:1445-8.

39. Collett D. *Modelling Survival Data in Medical Research*. 2nd edition, Chapman & Hall / CRC, Boca Rotan, Florida 2003.

40. Cox DR. Regression models and life-tables. *Journal of the Royal Statistical Society* 1972; 34:187-220.

## Figure legends

**Figure 1. Lin28 physically associates with BMP4 mRNA in Lin28-expressing cells.** (A) BMP4 mRNA is enriched in Lin28-containing RNPs in human ES cells as revealed by IP and deep sequencing<sup>19</sup>. RNA-Seq libraries were generated using RNAs captured by IP using anti-Lin28 or preimmune IgG. The libraries derived from Lin28 IP and preimmune IP samples were individually used for sequencing on an Illumina GAI platform. Approximately 10 million 75-nt reads were obtained from each IP sample, and these sequences were uniquely aligned to a combined database of the human genome and splice junctions and these read counts were further analyzed using normalized values to identify transcripts that were significantly different between the Lin28 IP and preimmune IP samples. The heights of the peaks indicate frequencies of the 75-nt sequence reads that match the particular exon regions of the genome marked as blue boxes at the bottom of the histograms. (B, C) BMP4 mRNA was enriched in Lin28-containing RNPs in PA-1 (B) and IGROV1 (C) cells by IP, followed by RNA extraction and RT-qPCR analysis. Relative abundance of the indicated mRNAs present in the anti-Lin28 vs. preimmune IP complexes are shown as relative fold enrichment. Error bars are mean  $\pm$  SD (n=3).

**Figure 2. Lin28 positively affects the expression of BMP4 at the protein level.** IGROV1 (A), A2780 (B), or PA-1 (C) cells were transfected with empty vector, FL-Lin28, siCon, or siLin28 as indicated. Proteins and RNAs were extracted 48 h post-transfection and levels determined by Western blotting and RT-qPCR analysis, respectively. Representative results of two independent experiments for each cell line are shown. For protein analysis, beta-tubulin was used as a loading control. Protein bands on Western gels were quantitated using the Bio-Rad Quantity One software. For RNA analysis, beta-tubulin mRNA was used for RNA level normalization, and beta-actin mRNA was used for non-target control for Lin28 effects. The levels of BMP4, beta-actin, and Lin28 mRNAs from empty vector- or siCon-transfected cells were arbitrarily set as 1. Error bars are mean  $\pm$  SD. (D) Reporter assays. Top, a

schematic drawing of human BMP4 transcript. The red rectangle represents open reading frame, with the 411-nt LRE highlighted in blue. Numbers are in nucleotides relative to the transcriptional start site of BMP4. Outlined beneath is a firefly luciferase reporter construct (FFL) with the green box representing its coding region and the thin line representing 3'-UTR. The position where the LRE was inserted is indicated. Bottom, luciferase assay results. The indicated constructs were each transfected into HEK293 cells that do not express endogenous Lin28, with increasing amounts of co-transfected FL-Lin28. Luciferase activities and FFL mRNA levels were measured 24 h post-transfection. Relative luciferase activities were presented after normalization against FFL mRNA levels. Luciferase activities from cells without FL-Lin28 transfected were arbitrarily set as 1. Numbers are mean  $\pm$  SD (n=3).

**Figure 3.** (A) Distributions of AQUA scores for Lin28 (left) and Oct4 (right) expressions in the Yale Ovarian Cancer Cohort. The range, mean and median values are indicated. (B) Examples of immunofluorescence of human epithelial ovarian cancer samples using antibodies specific for Lin28 (I, in red), Oct4 (V, in red), or cytokeratin (II and VI, in green), respectively. The Dapi stain (III and VII, in blue) indicates cell nuclear compartment. III, merge of cytokeratin and Dapi; VII, merge of Oct4 and Dapi; IV, merge of cytokeratin and Lin28; VIII, merge of cytokeratin and Oct4. Bar = 20  $\mu$ m. (C) Survival curves from a Cox proportional hazards regression analysis that included as covariates Lin28 and Oct4, along with their interaction term. Assessment of Lin28 and Oct4 expressions was performed in 3-fold redundancy.

**Figure 4.** A model for Lin28/BMP4/Oct4-mediated regulation in ovarian tumor.

**Supplementary Figure S1.** Predicted secondary structure of the 411-nt LRE from human BMP4 mRNA. The putative "A" bulges are indicated.

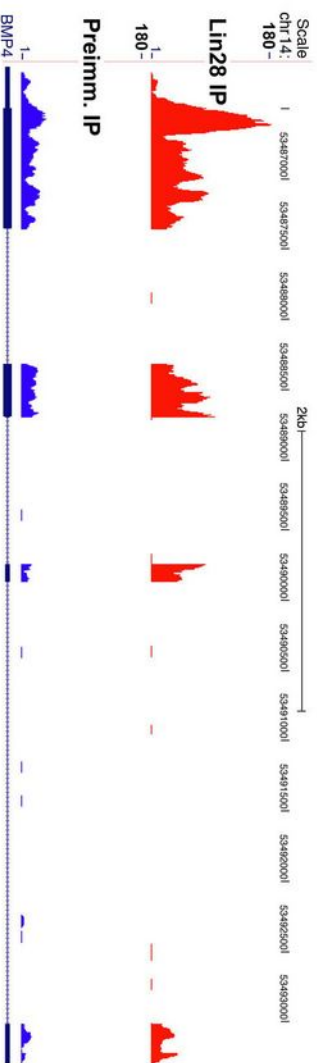
**Supplementary Table S1.** Characteristics of Yale Ovarian Cancer Cohort.

**Supplementary Table S2.** Interactions between Lin28 and Oct4 in progression free survival (PFS) and overall survival (OS) of patients with ovarian tumors. P-values are shown for null regression coefficients in univariate and multivariate Cox proportional hazards and accelerated failure time regression models for OS and PFS, respectively. The multivariate Cox model for OS was stratified by disease stage. The covariates (prognostic factors) used in the univariate and multivariate analyses included age at diagnosis, disease stage, tumor grade, tumor histology, bilateral involvement, category of specimen, and IHC labeling of Lin28 and Oct4. The multivariate models suggest that an interaction between Lin28 and Oct4 significantly affects both PFS and OS.

**Supplementary Table S3.** Co-expression of Lin28 and Oct4 at high levels associates with the least favorable prognosis. Estimated odds ratios (OR), hazard ratios (HR), and 95% confidence intervals (CI) for patients with no, medium or high Lin28 labeling and no, medium or high Oct4 labeling compared to patients with no Lin28 and high Oct4 labeling (referent group) derived from a multivariate disease-stage-stratified Cox model for OS and a log-logistic accelerated failure time model for PFS in patients with ovarian tumors. High=90<sup>th</sup> percentile of readable values of AQUA scores; Medium=the median (50<sup>th</sup> percentile) of readable values of AQUA scores; No=no readable values of AQUA scores.

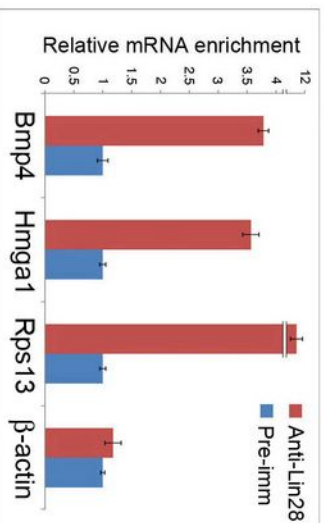
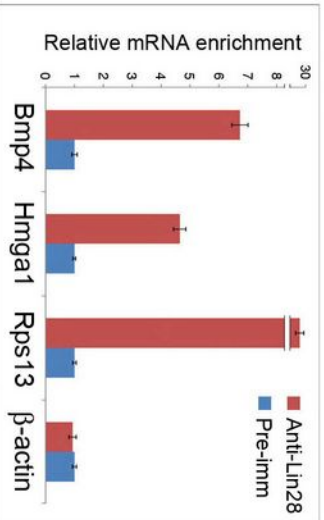
# A hESC

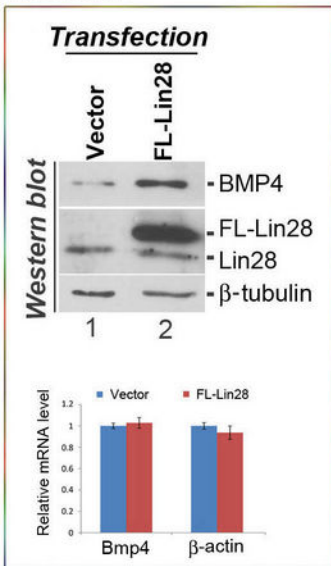
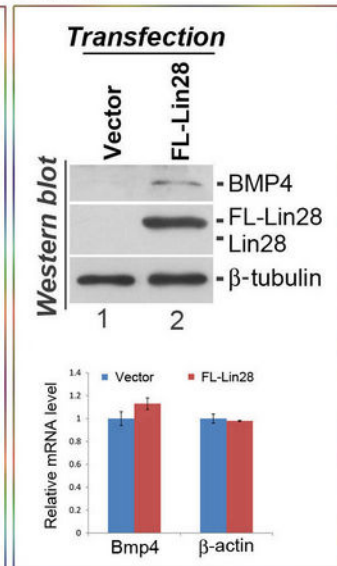
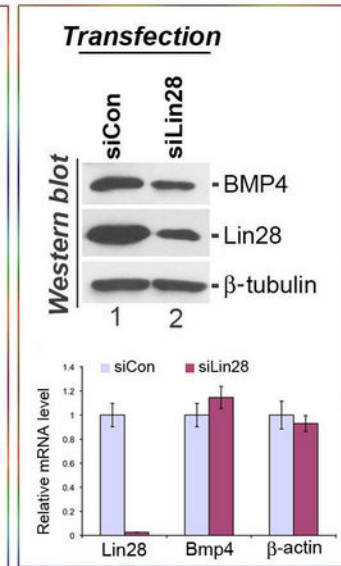
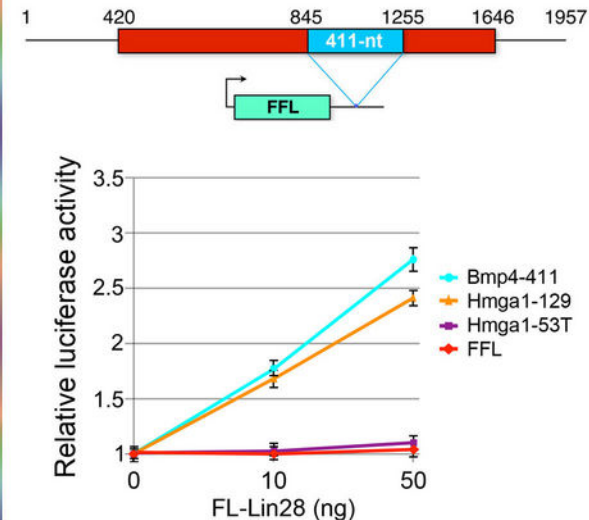
BMP4 mRNA enrichment = 3.9-fold

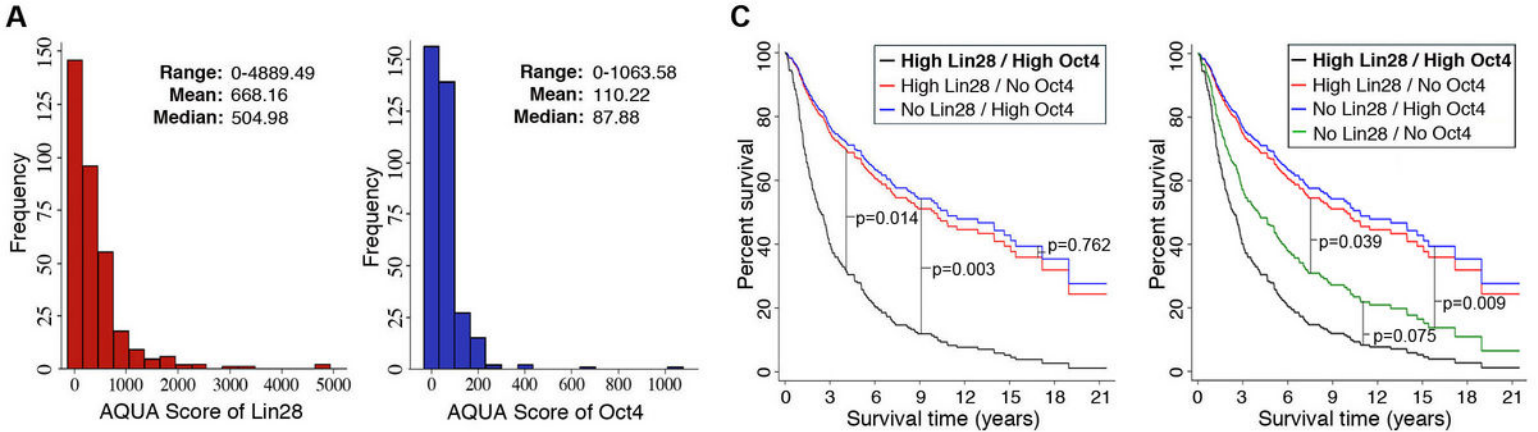


# B PA-1

# C IGROV1



**A** IGROV1**B** A2780**C** PA-1**D** HEK2993



**B**

